IOP Conf. Series: Materials Science and Engineering **966** (2020) 012011 doi:10.1088/1757-899X/966/1/012011

Destruction electrospark deposits during Joule heating of base metal

G E Trekin[1, 2] and O I Shevchenko[1]

[1] Ural Federal University named after the First President of Russia B N Yeltsin, Nizhniy Tagil Technological Institute, 59, Krasnogvardeyskaya str., Nizhniy Tagil, 622000, Russia

E-mail: [2] trekin1963@yandex.ru

Abstract. Electrospark coating deposited on the surfaces of machine parts is a common surface hardening method. Hard materials are normally used for depositing to improve wear resistance or other properties. In this investigation electrospark deposition intended for use as micro-alloying of welds by deposition on to the surface of the base metal and in this case it remelts completely. Intense heating and destruction occurs before remelting, which changes the chemical composition of the melt. The aluminum and titanium coatings is shown to deteriorate at 500 to 650 °C generating a liquid phase due to eutectic available in both metals in this temperature range. Most of titanium and aluminum oxidized at that. It is found that a solid layer, appears after electrospark depositing using both coatings. For aluminum coating, after high-temperature heating, a thicker white layer appears with the same microhardness level as that of the base metal, and a thin layer of partial decarburizing. Fusion sectors are detected in the titanium coating that are harder than the base metal and have a dendritic structure, followed by a thin zone of complete decarburization and quite an extended zone of partial decarburization.

1. Introduction

Metal deposition on the surface during electric spark discharging (electrospark deposition – ESD) occurs as a result of the cathode sputtering effect. In a molt pool on the anode appears cavern due to displacement by the spark discharge pressure. This molten area also receives, most likely, liquid drop going off the cathode. When the frequency of spark discharges is high, the melting zones of each discharge overlap and quite a solid coating is generated with cracks, since the cooling rate is very high. A zone, similar to a welding heat affected zone (HAZ), develops in the volume under the deposited layer. Intensive evaporation of metal from the spark discharge zone results in splashing and loss of the electrode metal [1–3]. Hard wear-resistant alloys are the most used for electrospark deposition [4, 5]. Layers of other materials deposited are used as scale and corrosion-resistant etc. [6–8]. Deposited aluminum and titanium were used as a micro-alloying layer for subsequent remelting, since the layer is about tenths of a millimeter thick and has cracks. The aluminum and titanium microalloying effect is beneficent for welded metal properties [9–12], so in this paper we studied changes in the near-surface volume after electrospark deposition and high-temperature heating before welding melting.

2. Materials and study methods

The electrospark deposition were conducted in the air environment using an experimental setup, designed in the Department of Metallurgical technology of NTI (branch) of UrFU, in the parameters that make formation (Table 1).

Table 1. Electrospark deposition parameters.

Electrode metal	d_{el} (mm)	I_{av} (A)	U_{av} (V)	E_{1imp} (kJ)	ν_{imp} (Hz)	ω_{el} (rpm)	V_{dep} (cm/s)
Al	40	18–22	75–80	4.85	300	50	6
Ti	20						

d_{el} – electrode diameter; I_{av} – average current; U_{av} – average voltage; E_{1imp} – pulse energy; ν_{imp} – pulse rate; ω_{el} – electrode rotation rate; V_{dep} – electrode traveling speed relative to workpiece.

The base metal are plates of the steel 20 (Table 2) with the cross section 3×25 mm and 250 mm long. The ESD layer was put on all planes through the entire length of the specimen.

Table 2. The nominal chemical composition of Steel 20, mass % [13].

C	Mn	Si	P	S	Cr	Ni	Cu	As
			not above					
0.17–0.24	0.3–0.65	0.17–0.37	0.25	0.04	0.035	0.25	0.25	0.08

The metallographic study was performed with a Zeiss Observer D1m microscope running under Thixomet software. Etching was carried out with Nital (6 %) solution for 20 s at the room temperature.

Microhardness indentation were made using a Future Tech FM 300 testing machine by the Vickers pyramid for a load 50 g over 50 s, at right angle to the specimen thickness. The results were processed by means of Excel and MathCAD software.

The distribution of chemical elements through the modified layer depth was investigated with a Phenom PRO scanning electron microscope.

The temperature was registered with K–type thermocouple. The thermal heating cycle was registered by connecting the thermocouple to a Zet 410 amplifier and a Zet 210 analog-to-digital converter (ADC). The current and voltage were recorded using the same setup equipped with current transformers and signal rectification and smoothing circuits.

The specimen was heated under fluxes AN 348 A and FSA ChT A 650 20/80 (table 3, 4) using a transformer TSD-1000-3 in parameters that make possible melting of the flux and heating of the workpiece above the flux melting temperature. and then it was cooled in water (Figure 1).

3. Results and discussion

The microstructure of the surface after electrospark deposition is a white high hardness layer with a lot of straight cracks. The aluminum layer surface is uneven, the titanium layer is more even (Figure 2 a, 3 a, 4 a, b). The thickness of the layer applied is 40–80 μm for an aluminum electrode, and about 30 μm for a titanium electrode. Behind the layer applied there is a HAZ with a ferritic structure having the thickness equal for both electrodes of about 100 μm (Figure 2 a, 3 a).

It is found, that the deposited layer completely disappears after Joule heating and cooling, and is replaced with a white low hardness layer. This is a dense layer with relatively smooth borders and a few pores and inclusions, for aluminum coating under both fluxes. A thin partial decarburizing layer is observed at some distance from the white layer, looking like a thicker ferrite border around the quenched structure areas (Figure 2 b, c and 4 c). This is an uneven thickness layer with melting areas of dendrite structure, for titanium coating. Complete and partial decarburizing zones occur behind the melting sectors, of which on zone is narrow, about 200 μm, and the other is of about 1 mm deep (Figure 3 b,c, 4 d).

The aluminum distribution through the thickness of the modified layer shows that aluminum diffuses approximately 68 μm deep after short electrothermal exposure and its maximum

concentration in the near-surface layer is 6–12 at. % (Figure 5 c). Titanium is distributed unevenly, in the melting area from 2 to 5 at. % with peaks up to 20 at. % (Figure 5 a, b), only peaks are also in other sections up to 20 at . %.

Table 3. The nominal chemical composition of AN-348-A flux, mass %.

Al_2O_3	MnO	CaO	MgO	CaF_2	Fe_2O_3	S	P
40–44	≤ 6	31–38	≤ 12	≤ 7	3–6	0.5–2.0	≤ 0.12

Table 4. The nominal chemical composition of FSA ChT A 650-20/80 flux, mass %.

The sum of oxides	Al_2O_3+CaO+ MgO	Al_2O_3	CaF_2
		min	
%	40	20	22

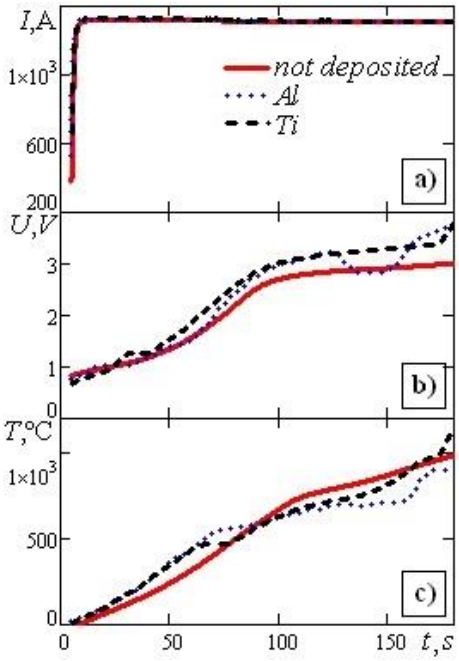

Figure 1. Changes in current (a), voltage (b) and temperature (c) during Joule heating under flux AN 348-A. Chemical element characters show the material of the electrode at ESD.

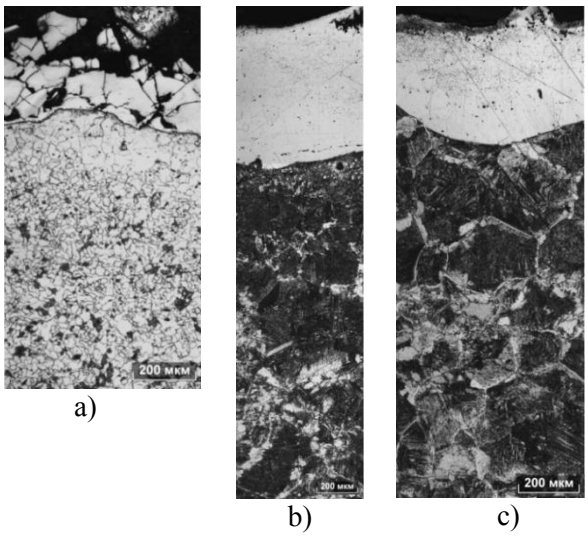

a) b) c)

Figure 2. Steel 20 surface layer microstructure aluminum deposit, after: a) – ESD; b) – ESD and Joule heating under FSA ChT A 650 20/80 flux; c) – ESD and Joule heating under AN 348-A flux, μm.

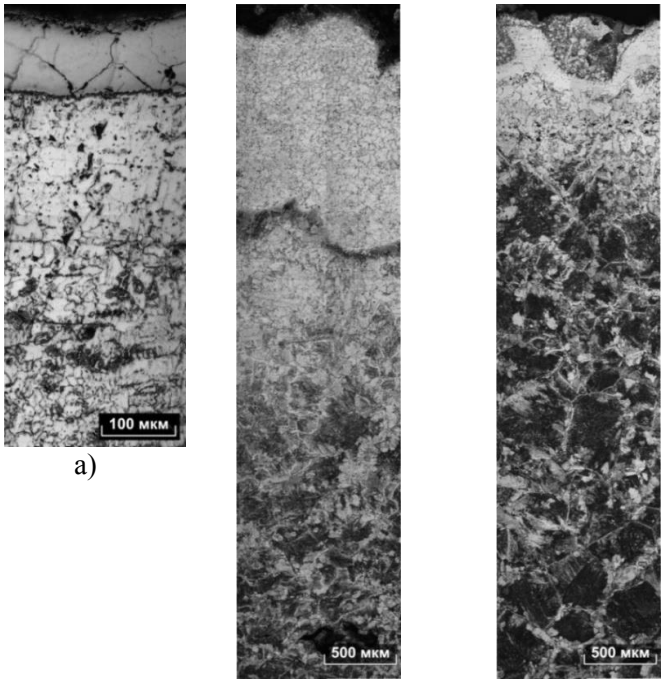

a) b) c)

Figure 3. Steel 20 surface layer microstructure titanium deposit after: a) – ESD; b) – ESD and Joule heating under FSA ChT A 650 20/80 flux; c) – ESD and Joule heating under AN 348-A flux, мкм = μm.

Iron to aluminum and iron to titanium diagram review [14–16], shows that intermetallides are likely to occur in the electrospark deposited layer, as they are detected during deposition of these materials [17], which is also confirmed high coating hardness and cracks. Generation nitrides and oxides should also not be ruled out, since the coating was deposited in an air environment. Small volumes of relatively pure electrode material are very likely. For example, the titanium content in its peak value reaches 72 at. % (Figure 5 a). When heated, the base metal interacts in the manner of diffusion penetration: on the base metal part, for both electrodes applied, it is α a solid solution with γ a region above 900 °C, on the aluminum part, eutectic is at 652 °C, on the titanium part, eutectic also is at 590 °C. Therefore, heating of both electrospark layers has to generate a liquid phase, which is actually observed, and the aluminum coating becomes smooth, while the titanium generates local melting sectors with a dendritic structure. This is confirmed by Figure 2 c, where the heating curves change in the range 500–650 °C for samples with an electrospark layer.

With increasing temperature afterwards, for the aluminum layer, the interaction develops in the form of diffusion path, oxidation on the surface side, local melting and subsequent dissolution on the fusion line side, so an aluminum oxide film and a thin film of solid solution with about 5 at. % get in the weld. Temperature increased in the titanium coating most likely results in titanium binding of carbon, which is evidenced by the decarburized zones that occur after electro-thermal exposure. The average content of titanium is about 7 at. % in the thin layer. Assuming, that the thickness of the titanium containing layer is approximately the same before and after high-temperature heating, then about 10 % of titanium is transferred to the base metal i.e. most of the titanium is transferred into the melt as an oxide.

Since the main structural changes occur before the melting point of the fluxes, their influence is basically weak, so the results differ insufficiently.

4. Summary

Thus, when the electrospark deposited layers by aluminum and titanium electrodes are heated to high temperature, the surface layer melts followed by diffusion redistribution of elements. A white deposit with a thin partial decarburized layer is generated in place of the aluminum electrospark coating.

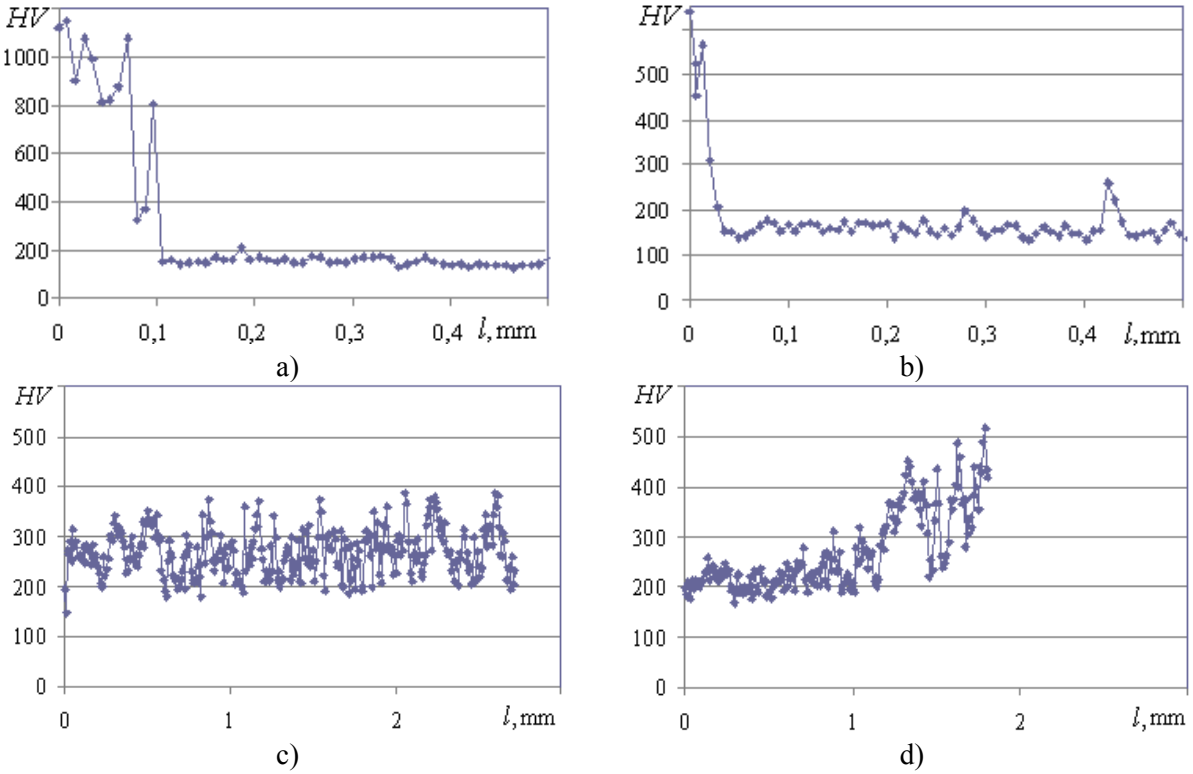

Figure 4. Microhardness (*HV*) distribution through the depth of the modified layer (*l*)
a, c – aluminum electrode; b, d – titanium electrode; a, b – after ESD;
c, d – after ESD and Joule heating under FSA ChT A 650 20/80 flux.

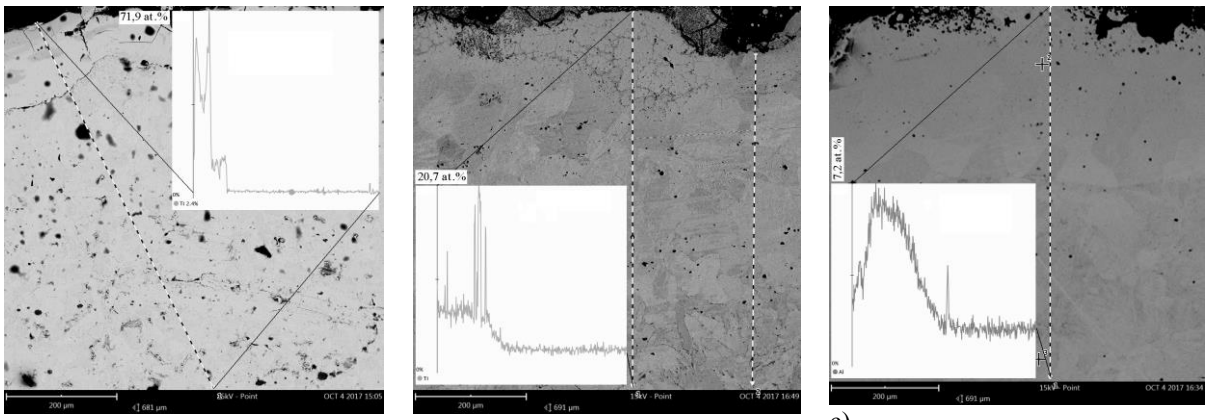

Figure 5. Titanium and aluminum distribution through the depth of the modified layer.
a, b – titanium electrode; c – aluminum electrode; a – after ESD; b, c – after ESD and Joule heating.

Local melting areas are generated in place of the titanium electrospark coating, followed by a thin complete decarburizing zone and about 1 mm of partial decarburizing. Most of the titanium and aluminum brought to the surface is oxidized and only max 10% remain in the electrospark modified layer after high-temperature heating.

References

[1] Ivanov V I, Burumkulov F Kh, Verkhoturov A D, Gordiyenko P S, Panin Ye S and Konevsov L A 2013 Formation of the surface layer on a low-carbon steel in electrospark treatment *Welding International* vol **27** issue **11** pp 903–6

[2] Sahin O and Ribalko A V 2011 Electrospark Deposition: Mass Transfer, Mass Transfer - Advanced Aspects Ed. Hironori Nakajima *InTech* Available online: http://www.intechopen.com/books/mass-transfer-advanced-aspects/electrospark-deposition-mass-transfer (accessed on 01.06.2020)
[3] Thamer A D, Hafiz M H and Mahdi B S 2012 Mechanism of Building-Up Deposited Layer during Electro-Spark Deposition. *Journal of Surface Engineered Materials and Advanced Technology* **2** pp 258–63
[4] Çakir A, Yilmaz M S, Ribalko A and Korkmaz K 2015 A Study on Modifcation of Micro-Alloy Steel Surfaces with Different Hard Materials Via Electro-Spark Deposition Method. *Proceedings of the 4th International Congress APMAS 2014, April 24-27, 2014, Fethiye, (Turkey) ACTA PHYSICA POLONICA A* vol **127** no **4** pp 1410–13
[5] Nikolenko S V, Verkhoturov A D, Syui N A and Kuz'michev E N 2016 Influence of electrospark discharge parameters on roughness and microabrasive wear of steel 45 surface after ESA by TiC-based electrodes. *Surface Engineering and Applied Electrochemistry* vol **52** issue **4** pp 342–9
[6] Jamnapara M I, Frangini St, Avtani D U and Nayak V S 2012 Microstructural studies of electrospark deposited aluminide coatings on 9Cr steels *Surface Engineering* vol **28** pp 700–4
[7] Jamnapara M I, Frangini St, Alphosa J, Chauhan N I and Mukherjee S 2015 Comparative analysis of insulating properties of plasma and thermally grown alumina films on electrospark aluminide coated 9Cr steels *Surface & Coatings Technology* **266** pp 146–50
[8] Kozyr A V, Konevtsov L A and Konovalov S V 2018 Research of heat resistance of the multilayer coating after electro-spark alloying of C45 steel Cr-Ni alloys *Letters on Materials* vol. **8** Issue **2** p 140-145.
[9] Bhadeshia H K and Svenson L E 1993 Modelling the evolution of microstructure in Steel weld metal *Mathematical Modelling of Weld Phenomena* eds H Cerjak, K E Easterling, Institute of materials (London) pp 109–82
[10] Trekin G E and Shevchenko O I 2015 Effect of aluminum electrospark sublayer and tempering temperature on the structure and qualities of low-carbon low-alloy welds *Bulletin of PNRPU Mechanical engineering, material science* vol **17** no **1** pp 112–8
[11] Wang J, Li G and Xiao A 2011 A Bainite-Ferrite Multi-Phase Steel Strengthened by Ti-Microalloying *Materials Transactions* vol **52** no **11** pp 2027–31
[12] Jorge J C F, Bott I S, Sauza L F G, Mendes M C, Araujo L S and Evans J M 2019 Mechanical and microstructural behavior of C-Mn steel weld deposits with varying titanium contents *J. Mater. Res. Techn.* **8 (5)** 4659–71
[13] Sorokin V G et al 2001 *Steels and alloys. Grade list: Ref.* ed. V G Sorokin and M A Gervasiev (Moscow: Intermet Engineering) p 608
[14] *Binary Alloy Phase Diagrams* 1986 ed by T B Massalski, J L Murray, L H Bennett and H Baker (ASM, Metals Park)
[15] Li X, Scherf A, Heilmaier M and Stein F 2016 The Al-Rich Part of the Fe-Al Phase Diagram *Journal of Phase Equilibria and Diffusion* vol **37** no **2** pp 162–73
[16] Okamoto H *Desk Handbook: Phase Diagrams for Binary Alloys* 2nd ed. ASM International® Materials Park, Ohio 44073-0002.
[17] Pyachin S A and Burkov A A 2015 Formation of intermetallic coatings by electrospark deposition of titanium and aluminum on a steel substrate *Surface Engineering and Applied Electrochemistry* **51:2** pp 118–24